International Journal of Pharmaceutics 495 (2015) 122–131

Contents lists available at ScienceDirect

International Journal of Pharmaceutics

journal homepage: www.elsevier.com/locate/ijpharm

Biodistribution and translational pharmacokinetic modeling of a human recombinant alkaline phosphatase

Esther Peters[a,b,1], Jasper Stevens[c,1], Jacques Arend[d], Zheng Guan[c], Willem Raaben[d], Peter Laverman[e], Andrea van Elsas[d], Rosalinde Masereeuw[b,f,2], Peter Pickkers[a,2,*]

[a] Department of Intensive Care Medicine, Radboud university medical center, PO Box 9101, Internal Mailbox 710, 6500HB Nijmegen, The Netherlandsc
[b] Department of Pharmacology and Toxicology, Radboud university medical center, PO Box 9101, Internal Mailbox 149, 6500HB Nijmegen, The Netherlands
[c] Centre for Human Drug Research, Zernikedreef 8, 2333CL Leiden, The Netherlands
[d] AM-Pharma, Rumpsterweg 6, 3981 AK Bunnik, The Netherlands
[e] Department of Radiology and Nuclear Medicine, Radboud university medical center, PO Box 9101, Internal Mailbox 756, 6500HB Nijmegen, The Netherlands
[f] Division of Pharmacology, Utrecht Institute for Pharmaceutical Sciences, Faculty of Science, Utrecht University, PO Box 80082, 3508 TB Utrecht, The Netherlands

ARTICLE INFO

Article history:
Received 23 June 2015
Received in revised form 24 August 2015
Accepted 26 August 2015
Available online xxx

Chemical compounds studied in this article:
Iodine-125 (PubChem CID: 104800)
Lipopolysaccharide (PubChem CID: 11970143)

Keywords:
Alkaline phosphatase
Pharmacokinetics
Sepsis
Acute kidney injury
Biodistribution
NONMEM

ABSTRACT

Clinical trials showed renal protective effects of bovine intestinal alkaline phosphatase (AP) in patients with sepsis-associated acute kidney injury (AKI). Subsequently, a human recombinant chimeric AP (recAP) was developed as a pharmaceutically acceptable alternative. Here, we investigated the biodistribution and pharmacokinetics (PK) of recAP and developed a translational population PK model. Biodistribution was studied during LPS-induced AKI in rats. Iodine-125-labeled recAP was primarily taken up by liver, spleen, adrenals, heart, lungs and kidneys followed by the gastro-intestinal tract and thyroid. Tissue distribution was not critically affected by endotoxemia. PK parameters were determined in rats and minipigs during IV bolus injections of recAP, administered once, or once daily during seven consecutive days. Plasma concentrations of recAP increased with increasing dose and disappeared in a biphasic manner. Exposure to recAP, estimated by AUC and C_{max}, was similar on days 1 and 7. Subsequently, population approach nonlinear mixed effects modeling was performed with recAP rat and minipig and biAP phase I PK data. Concentration versus time data was accurately described in all species by a two-compartmental model with allometric scaling based on body weight. This model provides a solid foundation for determining the optimal dose and duration of first-in-man recAP studies.

1. Introduction

Alkaline phosphatase (AP) is an endogenous membrane-bound enzyme, ubiquitously present in the human body. Four different iso-enzymes exist, the nomenclature of which refers to the tissue that each was originally identified in, namely germ cell, intestinal, placental and tissue-nonspecific (liver/bone/kidney) AP (Millan, 2006). Endogenous AP has several functions under physiological conditions; intestinal AP is involved in e.g. regulation of bicarbonate secretion, surface pH and lipid absorption (Lalles, 2014), while bone-derived AP plays a role in bone mineralization (Millan, 2006). Alternatively, there is increasing evidence that AP plays a significant role in regulating intestinal barrier function as well as host defense and innate immunity, in particular protection against acute inflammatory reactions induced by endotoxins, such as lipopolysaccharides (LPS) (Su et al., 2006; Verweij et al., 2004).

Abbreviations: AKI, acute kidney injury; AP, alkaline phosphatase; AUC, area under the curve; AUC_{0-t}, AUC from time 0 to time of last quantifiable serum concentration; $AUC_{0-\infty}$, AUC from time 0 to infinity; AUC_{0-24}, AUC from time 0 to time 24 h; biAP, bovine intestinal alkaline phophatase; CFB, change from baseline; CI, confidence interval; CL, clearance; C_{max}, maximum concentration; IV, intravenous; CWRESI, conditional weighted residuals with interaction; IIV, inter-individual variability; k_{el}, terminal elimination rate constant; LPS, lipopolysaccharide; OFV, objective function value; PK, pharmacokinetics; recAP, human recombinant alkaline phosphatase; RSE, relative standard error; $t_{1/2}$, terminal elimination half-life; t_{max}, time to reach C_{max}; TLC, thin layer chromatography; Vss, volume of distribution at steady state; %ID/g, % of injected dose per g of tissue; ^{125}I, Iodine-125.

* Corresponding author. Fax: +31 24 36 68058.
E-mail address: peter.pickkers@radboudumc.nl (P. Pickkers).
[1] These authors contributed equally to this work.
[2] These authors share senior authorship.

http://dx.doi.org/10.1016/j.ijpharm.2015.08.090
0378-5173/

LPS are embedded in the outer membrane of Gram-negative bacteria and are considered one of the principal biological substances causing sepsis (Cohen, 2002). Sepsis is characterized by the release of various pro-inflammatory molecules from damaged necrotic and apoptotic cells, exerting toxic effects, including ATP (Eltzschig et al., 2012). Likely, AP exerts protective effects through the dephosphorylation of detrimental molecules, including LPS and extracellular ATP, thereby reducing the inflammatory response (Peters et al., 2014). The protective effects were demonstrated in several animal models of systemic inflammation. In mice, treatment with placental and intestinal AP improved survival rates, reduced fever and attenuated serum nitric oxide levels during *Escherichia coli*-induced inflammation, and reduced systemic inflammation and organ damage induced by cecal ligation and puncture (Beumer et al., 2003; van Veen et al., 2005; Verweij et al., 2004). In addition, treatment with intestinal AP attenuated systemic cytokine levels in sheep and piglets with septic shock caused by fecal peritonitis and LPS injection, respectively (Beumer et al., 2003; Su et al., 2006).

Subsequently, the anti-inflammatory role of AP was investigated in critically ill patients suffering from sepsis-associated acute kidney injury (AKI) (Heemskerk et al., 2009; Pickkers et al., 2012), a condition with substantial mortality (Oppert et al., 2008). Prior to two exploratory phase IIa clinical trials, conducted with bovine derived intestinal AP (biAP), the safety of this enzyme was evaluated in a phase I trial (Pickkers et al., 2009). BiAP administration in healthy male volunteers did not raise safety concerns and anti-drug antibodies were not detected. According to the clinical data available from two phase IIa studies, biAP infusion improved kidney function in patients with sepsis-associated AKI and showed a trend towards prevention of AKI development in patients diagnosed with sepsis, but that had no signs of AKI at inclusion (Heemskerk et al., 2009; Pickkers et al., 2012). The precise mechanism of action underlying these protective effects remains to be elucidated further, but it is known that endogenous AP is lost from the brush border membrane of proximal tubular epithelial cells in the kidney following an ischemic insult, while AP levels in urine are increased (Coux et al., 2002; Khundmiri et al., 1997).

Although biAP administration showed promising effects during sepsis-associated AKI, application of animal-derived enzymes in humans is not warranted as bovine spongiform encephalopathy (BSE)-free sources of bovine-derived enzyme are difficult to obtain. Also, repeatedly administering animal-sourced AP is likely to provoke immune reactions. As an acceptable alternative to bovine-sourced AP for human application in sepsis-associated AKI, a human recombinant chimeric AP (recAP) was developed by replacing the crown domain of a human intestinal AP with the crown domain of human placental AP, resulting in a stable and highly active enzyme (Kiffer-Moreira et al., 2014). In validation studies, enzymatic properties and substrate specificity of biAP and recAP were comparable, but recAP was found to be more temperature-stable compared to biAP (Kiffer-Moreira et al., 2014).

Insight into the pharmacokinetic (PK) properties of biAP in human subjects could support understanding the translational PK properties of recAP, which will ultimately help to predict the human PK of recAP. Subsequently, simulations of plasma PK profiles will improve the design of first-in-man recAP studies. Therefore, the aim of this study was to analyze clinical PK studies with biAP and preclinical PK studies with recAP to investigate recAP PK properties and translate these to a putative clinical application. In addition, to understand the relative distribution into various organs, a biodistribution study was performed with iodine-125 (^{125}I)-labeled recAP in rats during endotoxemia-induced AKI.

2. Materials and methods

2.1. Biodistribution study

2.1.1. Animals

For the biodistribution study, male Sprague–Dawley (SD) rats (Charles River Laboratories, L'Arbresle, France; $n = 43$), weighing 285–329 g, were housed under routine laboratory conditions at the Preclinical Image Centre of the Central Animal Laboratory at the Radboud university medical center (Nijmegen, The Netherlands). For the pharmacokinetic studies, male SD rats (Charles River Laboratories, Portage, Michigan; $n = 27$), weighing 330–372 g, and male Göttingen Minipigs (Marshall BioResources, North Rose, NY; $n = 18$), weighing 7–13 kg, were housed under routine laboratory conditions at MPI Research (Mattawan, MI). Water was available ad libitum. Standard laboratory chow was available ad libitum to rats and was offered to minipigs twice daily via rationated feeding, except during fasting periods. Animal experiments were performed according to the National Institutes of Health guidelines and protocols were approved by the institutional review board for animal experiments.

2.1.2. ^{125}I labeling

For the biodistribution study, recAP (AM-Pharma BV, The Netherlands) was radiolabeled with ^{125}I using the chloramine-T procedure (Greenwood et al., 1963). Briefly, 2 mg recAP (3873 U/ml), Na ^{125}I solution (37 MBq in 10 μL; PerkinElmer, Groningen, The Netherlands), 100 μL 5 mM Tris Buffer (pH 8.0; Sigma–Aldrich, Zwijndrecht, The Netherlands) and 14 μL of freshly prepared chloramine-T solution (10 mg/ml in sterile water; Sigma–Aldrich) were added into a 1.5 mL Lo-Bind Eppendorf tube. Reaction was allowed to stir for 1 min at room temperature. The labeling reaction was quenched by addition of 30 μL tyrosine solution (10 mg/mL in water; Sigma–Aldrich) and purified by gel filtration (PD10 column; GE Healthcare, Hoevelaken, The Netherlands) eluted with saline (0.9%). Fractions of 0.5 mL were collected and radioactivity in each fraction was measured in a dose calibrator (Capintec, Ramsey, NJ). Fractions containing the desired radio-iodinated product were pooled. Radiochemical purity was evaluated by thin layer chromatography (TLC) on silica gel-coated instant TLC strips (ITLC-SG; Agilent Technologies, Palo Alto, CA) with 10% trichloroacetic acid (Sigma–Aldrich) as eluent. Enzyme activity was verified by the AP colorimetric assay kit (Abcam, Cambridge, United Kingdom) and shown to be essentially unchanged after radiolabeling. The solution of radiolabelled ^{125}I-recAP was then diluted to ~1 mg/mL with saline. The ^{125}I-recAP dose prepared in saline for injection contained 200 U/kg enzyme activity (approximately 111 μg, 444 kBq per animal). Radiochemical purity of all preparations was >99%.

2.1.3. Study design

Rats received an IV bolus of 10 mg/kg LPS (*E. coli* 0127:B8; Sigma–Aldrich, Zwijndrecht, The Netherlands; dissolved in saline; group G8-G14), or placebo (saline, group G1–G7; $n = 3$ per group; group G14: $n = 4$; Supplemental Table 1) two h preceding the IV bolus injection of 111 μg ^{125}I-recAP (444 kBq, ~200 U/kg; $n = 43$). This dose of LPS demonstrated induction of renal nitric oxide and inducible nitric oxide synthase expression levels (Berg et al., 2007), resulting in endotoxemia-induced AKI (Heemskerk et al., 2006). Blood was collected at 2, 10, 15 and 30 min, 1, 2, 3, 4, 6, 12 and 24 h post ^{125}I-recAP injection through a tail vein puncture using a Multivette (Sarstedt, Etten-Leur, the Netherlands). At 10 min, 30 min, 1, 2, 4, 6 or 24 h post ^{125}I-recAP injection, animals were euthanized by CO_2 inhalation, followed by exsanguination by cardiac puncture. Twelve hour after ^{125}I-recAP injection, the group of rats to be sacrificed at 24 h received 1 mL saline (subcutaneous)

to prevent dehydration. From each animal, the adrenal gland, fat, heart, kidney, large and small intestines, liver, lung, muscle, stomach, spleen, and thyroid were harvested. Tissue and blood samples were weighed and radioactivity, expressed as percentage of injected dose per g of tissue (%ID/g), was measured using Wizard^2 Gamma Counter (2480 model, Perkin Elmer, Groningen, The Netherlands). AP enzyme activity was determined in serum samples by the AP colorimetric assay kit according to manufacturer's protocol (dilution range: 1:12–1:400). One rat was excluded from group G11 (see Supplementary Table 1) due to failed ^{125}I-recAP injection. Data is represented as mean (SD). Statistical differences between groups were estimated by an unpaired Student's *t*-test, differences between groups over time were estimated by two-way ANOVA with post-hoc comparisons using Bonferroni's multiple comparison test.

2.2. Pharmacokinetic biAP study

Data describing human PK properties of biAP were previously published (Pickkers et al., 2009).

2.3. Pharmacokinetic recAP studies

In the first part, rats and minipigs received a single intravenous (IV) dose of 0.08 (50 U/kg), 0.32 (200 U/kg) or 1.6 mg/kg (1000 U/kg) recAP at a dose volume of 2.5 mL/kg, diluted in saline ($n = 3$ per group; Table 1). Blood was collected into tubes containing lithium heparin and aprotinin from the jugular vein predose and 2.5 min, 5 min, 15 min, 30 min, 1, 2, 4, 8, 12, 24 and 48 h postdose. In rats, the jugular vein was cannulated and following each blood sample the volume collected was replaced by sterile saline. In the second part, rats and minipigs received IV doses of respectively 0.08 (50 U/kg), 0.32 (200 U/kg) or 1.6 mg/kg (1000 U/kg) recAP, once daily for 7 consecutive days, at a dose volume of 2.5 mL/kg, diluted in saline (Table 1). In rats ($n = 6$ per group), blood was collected from the jugular vein predose and 2 min, 4 min, 10 min, 30 min, 1, 6 and 24 h postdose at day 1 and 7, and prior to dosing at day 3–6 (alternating sampling per time-point in two cohorts of $n = 3$). In minipigs ($n = 3$ per group), blood was sampled from the anterior vena cava 2.5 min, 5 min, 15 min, 30 min, 1, 4, 12, and 24 h postdose at day 1 and 7, and prior to dosing at day 3–6. Blood was collected in tubes containing lithium heparin and aprotinin. Animals were observed at least twice a day for morbidity, mortality, injury and availability of food and water. A detailed clinical examination, including but not limited to evaluation of skin, fur, eyes, ears, nose, oral cavity, thorax, abdomen, external genitalia, limbs and feet, and respiratory, circulatory, autonomic and nervous system effects, was conducted predose and just prior to euthanasia. After the final blood sample, rats were euthanized by CO_2 inhalation, followed by exsanguination by puncturing the abdominal vena cava. Minipigs were euthanized via an IV overdose of sodium pentobarbital under Telazol sedation (intramuscular). PK parameters, determined from serum concentration-time data for recAP, included maximum concentration (C_{max}), time to reach C_{max} (t_{max}), terminal elimination half-life ($t_{1/2}$), area under the plasma concentration-time curve from time 0 to infinity ($AUC_{0-\infty}$), time 0 to 24 h (AUC_{0-24}), time 0 to 48 h (AUC_{0-48}), clearance (CL) and volume of distribution at steady state (Vss). RecAP bioanalysis was performed using a validated electrochemiluminescent ligand-binding procedure (lower limit of quantitation: 15.6 ng/ml and 25.6 ng/ml for rat and minipig serummatrix, respectively). The activity of AP was measured by routine laboratory analysis. All PK data, represented as mean (SD), were summarized in tabular or graphical form and descriptive statistics were given. PK parameters were determined by non-compartmental methods using WinNonlin^{TM} Professional, Version 6.1 (Pharsight Corporation, Mountain View, CA).

2.4. Population PK model development

Population approach nonlinear mixed effects modeling was performed with the software package NONMEM (version 7.2.0, Icon Development Solutions, Ellicott City, MD). First, models of biAP and recAP were built separately, where after an integrated model with all biAP and recAP data was developed. Nonlinear mixed effect modeling considered repeated PK observations as a function of time in a population of individuals. The model to describe these observations adopted a common structural model and distribution of residuals, while allowing the parameters in the model to vary between individuals. The location (typical value or fixed effect) and spread between individuals (variability or random effect) were estimated for the model parameters by fitting the model to the data by minimizing an objective function based on the log likelihood ($-2 \times$ LL). The random effects structure that was applied included a residual error distribution and distributions for the inter-individual variability of the PK parameters. Additive, proportional or combined residual error structures were investigated, while log-normal distribution for the inter-individual variability was assumed. The distribution of these individual parameters were compared per dataset with the theoretical distribution based on the population values (median and 80, 90, or

Table 1
Dosing schedule of pharmacokinetic studies.

	biAP	recAP	IV loading dose (U/kg)		IV infusion	
	$n = 29$	$n = 36$	Day 1	Day 2–7	Dose (U/kg/24 h)	Duration (h)
Animal cohort – Part 1[a]		18[a]				
Group 1	–	3	50	–	–	–
Group 2	–	3	200	–	–	–
Group 3	–	3	1000	–	–	–
Animal cohort – Part 2[a]		18[a]				
Group 1	–	3[b]	50	50	–	–
Group 2	–	3[b]	200	200	–	–
Group 3	–	3[b]	1000	1000	–	–
Human cohort (Pickkers et al., 2009)	29					
Group 1	6	–	7.5[c]	–	–	–
Group 2	6	–	22.5[c]	–	–	–
Group 3	6	–	67.5[c]	–	–	–
Group 4	6	–	–	–	200	24
Group 5	5	–	67.5[c]	–	177.5	72

[a] The studies of the animal cohort were conducted in rats and minipigs.
[b] Alternating sampling per time-point in two cohorts of $n = 3$.
[c] Loading dose was administered over 10 min. BiAP, bovine intestinal alkaline phosphatase; RecAP, human recombinant alkaline phosphatase.

95% prediction interval) and residual variability and shrinkage were reported, which were considered acceptable when below 35%. Finally, various types of variance–covariance matrices were tested for the inter-individual variability. In order to find the simplest model adequately describing PK observations, different models were compared with increasing complexity in the structural model and the number of random effects. The likelihood ratio test was used, which compares the difference between −2*log-likelihoods of the models (difference in objective function value, ΔOFV) to a Chi-square distribution with degrees of freedom corresponding to the difference in number of parameters between the two models. Hence, with a difference of at least 6.63 points ($P < 0.01$) the model with one additional parameter was preferred over its parent model.

Graphical analysis was another tool used to help assessing differences between models. These goodness-of-fit plots included: (1) population predicted and individual predicted vs. observed concentrations, (2) conditional weighted residuals with interaction (CWRESI) vs. predicted concentration and vs. time, where most CWRESI should be normally distributed around zero and be within the acceptance criterion of −2 to 2, (3) frequency distribution of the CWRESI, (3) frequency distributions of the post hoc individual estimates of η's, and (4) correlation plots with their Pearson's correlation coefficient of all parameters with inter-individual variability (Pearson, 1895). The uncertainty of parameter estimates was determined by the relative standard error (RSE; standard error/parameter estimate × 100%) and considered acceptable when the RSE was less than 50%. For the parameter estimates of inter-individual variability (IIV), shrinkage was reported as a measure of identifiability and considered acceptable when below 35%. The translational population PK component focussed on identifying a compartmental structural model to describe the preclinical- and clinical datasets of biAP simultaneously by allometric scaling between species; the pharmacokinetic parameters CL and volume of distribution were scaled, based on bodyweight, according to Eq. (1),

$$\theta_i = \theta_{TV} \times \left(\frac{BW_i}{70}\right)^{\text{exponent}} \quad (1)$$

where θ_i is the PK parameter for CL or volume of distribution for the ith individual, θ_{TV} its typical population value and BW_i the bodyweight of the ith individual in kg (normalized for the typical bodyweight of humans; 70 kg). The exponents were set at 0.75 and 1 for CL and volume of distribution, respectively (Boxenbaum, 1982). The biAP model was employed to describe the population PK of recAP in rats and minipigs, using the allometric scaling factors discovered for biAP. To investigate the possibility of difference in PK properties between biAP en recAP, potential differences were quantified in terms of a scaling parameter for each PK parameter. The scaling parameters were accepted when the 95% confidence intervals did not overlap with zero and utilized to translate the biAP PK in humans to a prediction of recAP PK in

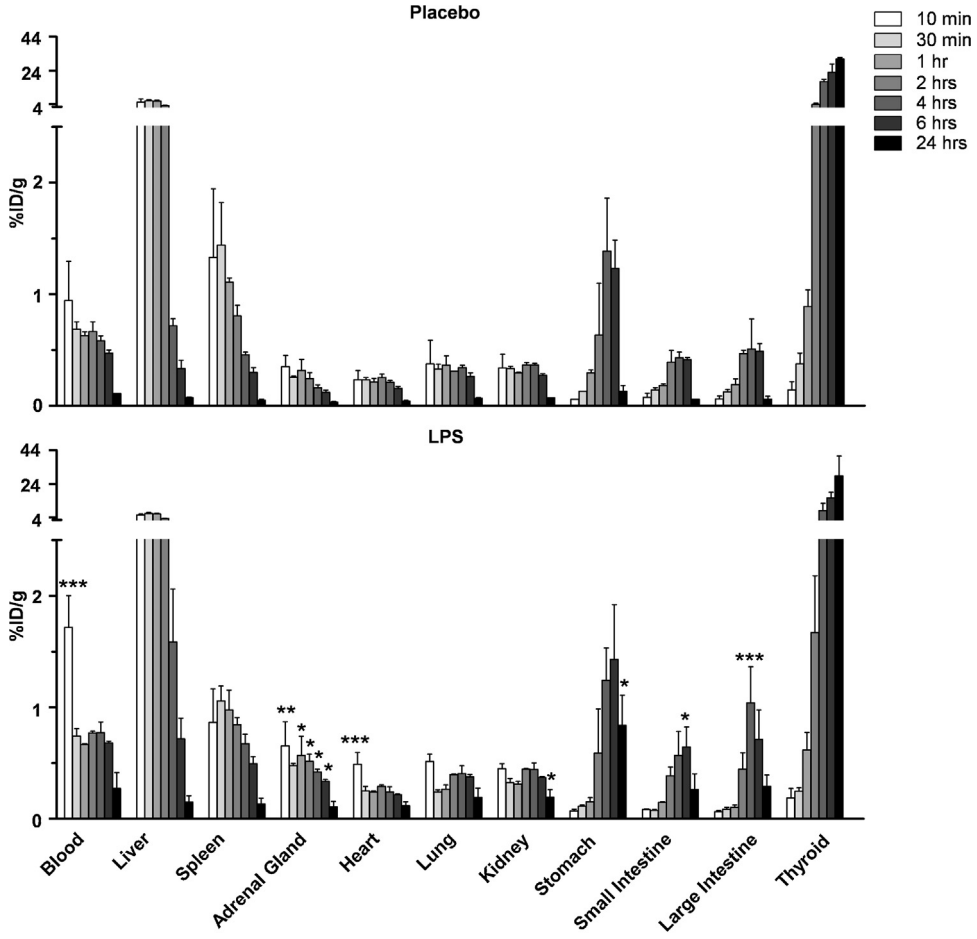

Fig. 1. Tissue distribution of ^{125}I-recAP in rats during endotoxemia. Rats were pretreated for 2 h with LPS (lower panel) or placebo (upper panel), followed by the administration of an IV bolus injection of ^{125}I-recAP. Animals were sacrificed at several time-points post ^{125}I-recAP injection and radioactivity, expressed as percentage of injected dose per g of tissue, was determined. Data is expressed as mean with standard deviation. $N = 3$ per time-point, except for adrenal gland at $t = 30$ min ($n = 2$; LPS) and for all organs at $t = 2$ (LPS); $n = 4$ for $t = 24$ h (LPS). $^*P < 0.05$, $^{**}P < 0.01$, $^{***}P < 0.001$ compared to placebo, determined by two-way ANOVA. RecAP, human recombinant alkaline phosphatase; IV, intravenous; LPS, lipopolysaccharide; ^{125}I, Iodine-125; %ID/g, % of injected dose per g of tissue.

humans. Data analysis using the approach described was performed using NONMEM. The first-order method with conditional estimation and interaction (FOCEI) was used for the maximum likelihood parameter estimation. Additionally, R 2.12.0 was used for graphical presentation, evaluation of goodness of fit, covariate selection, and model evaluation (R, 2010). The analyses closely followed the FDA and EMA guidelines for performing and reporting population pharmacokinetic analyses (EMA, 2007; FDA, 1999).

3. Results

3.1. Biodistribution of recAP

The biodistribution of ^{125}I-recAP (111 μg, ~200 U/kg) was investigated in rats, pretreated with LPS (10 mg/ml) or placebo to determine the effect of systemic inflammation. Blood samples were collected and organs were harvested at several time-points after ^{125}I-recAP administration (Supplementary Table 1). LPS treatment caused shivering, diarrhea, pilo-erection, polyuria, reduced spontaneous activity, and mean weight loss (SD) after 24 h (Placebo: 2 (1.6)% vs. LPS: 14 (0.8)%; $P < 0.05$), consistent with the presence of systemic inflammation. Mean serum ^{125}I-recAP radioactivity rapidly decreased after infusion and was higher in the LPS-group 2 and 10 min after injection compared to the placebo group (2 min: Placebo: 3.1 (0.3) vs. LPS: 4.2 (1.0) %ID/g; $P < 0.001$; 10 min: Fig. 1 and Supplemental Table 2). Within the first 2 h after ^{125}I-recAP administration, relative uptake was highest in the liver, followed by the spleen, adrenal gland, heart, lung and kidney (Fig. 1 and Supplemental Table 2). LPS treatment increased accumulation in the heart 10 min post-^{125}I-recAP injection ($P < 0.001$), in the kidney 24 h post administration ($P < 0.05$) and in the adrenal gland at several time-points ($P < 0.05$; Supplemental Fig. 1). In addition, increased distribution was observed to the gastro-intestinal tract and thyroid gland (Fig. 1 and Supplemental Table 2), which was more pronounced in septic animals compared to placebo at 4 h (large intestine, $P < 0.001$), 6 h (small intestine, $P < 0.05$) and 24 h (stomach, $P < 0.05$) post injection (Supplemental Fig. 1). The absolute median accumulation in organs after LPS compared to placebo increased by a factor of 2.1 [1.6–6.4] (Fig. 1). Accumulation in muscle and fat was negligible at all time-points (Supplemental Table 2).

3.2. RecAP pharmacokinetics in rats

PK parameters, as presented in Table 2, were determined in rats during IV bolus injections of 50 U/kg, 200 U/kg or 1000 U/kg recAP ($n = 3$), administered once, or once daily during seven consecutive days. Repeated administration of recAP was well tolerated and no test article-related changes in morbidity, mortality, clinical observations and food consumption were noted. Plasma concentrations of recAP increased with increasing dose and disappeared in a biphasic manner on days 1 and 7. After a single dose, $AUC_{0-\infty}$, AUC_{0-48} and $AUC_{0-tlast}$ increased more than in proportion to dose between 50 and 200 U/kg and in approximate proportion to dose between 200 and 1000 U/kg. C_{max} increased in approximate proportion to dose over the entire dose range. CL was slightly higher and Vss and $t_{1/2}$ were slightly lower at 50 U/kg than at the two higher doses. RecAP was not detectable after 12 h at the lowest dose. Following seven days of dosing, $AUC_{0-\infty}$, AUC_{0-24} and C_{max} increased in approximate proportion to dose over the entire dose range. T_{max} was 2.5 min (first sampling time) at all dose levels on day 1 and day 7 and CL, Vss and $t_{1/2}$ were similar across the dose range on both days. AUC_{0-24} and C_{max} were similar on days 1 and 7; accumulation ratios ranged from 0.528 to 1.04. At termination, there were minimal to marked dose-dependent elevations in AP enzyme activity in all treatment groups relative to expected ranges. Relative to rats receiving 50 U/kg, terminal AP activity was elevated 1.5-fold and 4.6-fold in animals receiving 200 and 1000 U/kg, respectively. These changes were anticipated and considered

Table 2
PK parameters after non-compartmental analysis.

	Part	Dose (U/kg)	C_{max}[f] (ng/mL)	AUC_{0-24}[g,h] (h ng/mL)	$AUC_{0-\infty}$[g] (h ng/mL)	CL[i] (mL/min/kg)	$t_{1/2}$ (h)	Vss[j] (mL/kg)
Rats[a]	1	50	1100 (155)	1730 (240)	1840 (268)	0.74 (0.12)	5.7 (1.2)	321 (46)
		200	6740 (695)	9590 (1370)	10200 (1470)	0.53 (0.07)	12.7 (1.2)	443 (47)
		1000	39900 (4760)	48200 (9260)	51700 (9910)	0.53 (0.10)	13.5 (2.2)	427 (84)
	2[c,k]	50	1910	3080	–	0.35	9.3	260
		200	7100	9330	–	0.50	8.3	285
		1000	37100	43500	–	0.48	9.7	381
Minipigs[a]	1	50	947 (249)	3880 (651)	4480 (782)	0.30 (0.06)	15.9 (4.1)	386 (71)
		200	3700 (179)	18400 (1140)	32800 (3550)	0.16 (0.02)	44.3 (10.4)	574 (90)
		1000	24300 (3160)	88400 (6180)	203000 (111000)	0.16 (0.08)	60.8 (43.1)	603 (220)
	2[c]	50	814 (85)	7940 (1180)	–	0.10 (0.06)	24.1 (13.2)	157 (22)
		200	4390 (173)	37700 (1920)	–	0.05 (0.01)	38.2 (3.4)	166 (7)
		1000	28300 (1380)	151000 (5680)	–	0.07 (0.02)	38.1 (20.9)	199 (37)
Humans[b] (Pickkers et al., 2009)		7.5	82.8 (17.4)	–	364.4 (175.7)	1.6 (0.8)	12.2 (8.6)	–
		22.5	167.3 (45.6)	–	405.7 (176.5)	4.1 (1.1)	5.0 (1.0)	–
		67.5	501.2 (86.6)	–	642.5 (192.4)	7.8 (1.9)	3.8 (0.3)	–
		200[d]	61.8 (13.2)	1282.3 (345.3)	2005.1 (375.7)	7.2 (1.5)	11.9 (5.9)	–
		177.5[e]	272.4 (33.4)	1084.3 (167.4)	3472.8 (574.9)	4.7 (0.8)	8.3 (0.7)	–

[a] recAP treatment.
[b] biAP treatment.
[c] Day 7.
[d] Per hour during 24 h.
[e] Per hour during 72 h, preceded by loading dose (67.5 U/kg).
[f] U/L for biAP.
[g] U h/L for biAP.
[h] AUC_{0-48} for part 1.
[i] Per 1.73 m^2 (L/h) for biAP.
[j] Determined for recAP treatment only.
[k] Alternating sampling per time-point in two cohorts of $n = 3$. Data presented as mean (SD).

test-article related. In addition, during endotoxemia, while AP enzyme activity levels were significantly increased 2 min after injection compared to placebo (Placebo: 2273 (1614) vs. LPS: 4263 (1090) U/L; $P < 0.001$), no differences were observed between terminal $t_{1/2}$ (Placebo: 16.5 (2.8) vs. LPS: 19.9 (2.6) h; NS).

3.3. RecAP pharmacokinetics in minipigs

Subsequently, PK parameters were investigated in minipig during IV bolus injections of 50 U/kg, 200 U/kg or 1000 U/kg recAP ($n = 3$), administered once, or once daily during seven consecutive days (Table 2). RecAP administration was well tolerated without treatment-related effects on morbidity and mortality. Plasma recAP concentrations increased with increasing dose and disappeared in a biphasic manner (Fig. 2). Plasma AP enzyme activity levels followed a similar pattern as plasma recAP concentrations; after reaching a maximum, AP activity decreased rapidly followed by a slower decline (Fig. 2), and mean AP activity-time profiles displayed a dose-dependent increase in AP activity following administration of increasing doses of recAP.

After a single dose, recAP PK parameters $AUC_{0-\infty}$, AUC_{0-48} and $AUC_{0-tlast}$, C_{max}, Vss and $t_{1/2}$ in minipigs followed a comparable pattern to those in rats. Following seven-day recAP treatment, all animals had mild elevations in activated partial thromboplastin time (APTT; up to 1.4-fold) and mild elevations in urine pH relative to pretest values (pH range: 7.0–8.5 vs. 5.5–7.5). Based on the small magnitude, these changes are considered to be of minimal biologic relevance. RecAP $AUC_{0-\infty}$, AUC_{0-24} and C_{max} increased more than in proportion to dose between 50 and 200 U/kg and in approximate proportion to dose between 200 and 1000 U/kg on days 1 and 7. T_{max} occurred at the first or second sampling time. CL was higher at 50 U/kg than at the two higher doses on Days 1 and 7. Vss and $t_{1/2}$ were similar across the dose range on day 1 and day 7. CL and Vss were slightly reduced on day 7 as compared to day 1; $t_{1/2}$ was similar on both days. Exposure to recAP, as estimated by AUC and C_{max}, was similar on days 1 and 7; mean accumulation ratios ranged from 1.05 to 2.39. AP enzyme activity $AUC_{0-\infty}$, AUC_{0-24} and C_{max} increased in approximate proportion to recAP dose between 50 and 1000 U/kg/day on day 1 and day 7 (data not shown). T_{max} and $t_{1/2}$ did not vary with dose or duration of recAP treatment (data not shown).

3.4. Pharmacokinetic modeling

As initial assessment of the data suggested that a two-compartment PK model with first-order elimination would be required to describe the concentration versus time data, model development started with this model. Data below the lower limit

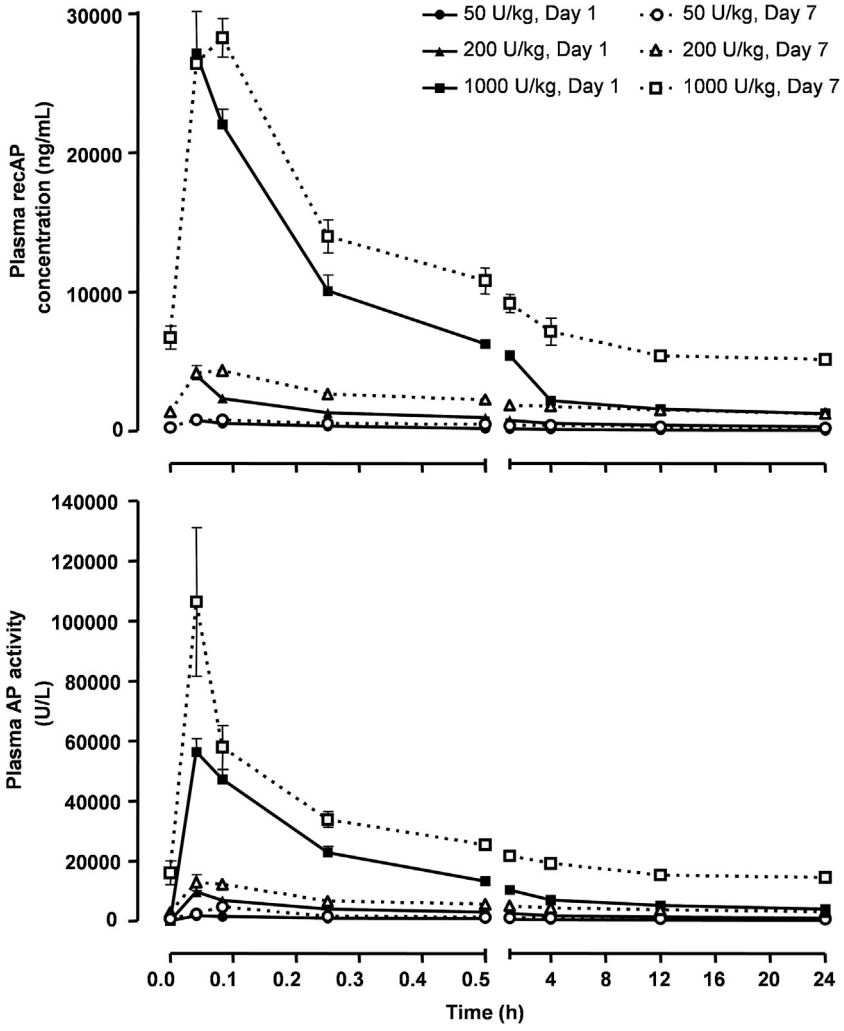

Fig. 2. Plasma recAP and AP activity in healthy minipigs on day 1 and day 7. Serum recAP concentrations (upper panel) and AP activity levels (lower panel) were determined several time-points after IV bolus injection of recAP, once daily for 7 consecutive days. Data is expressed as mean with standard deviation ($n = 3$ per group). RecAP, human recombinant alkaline phosphatase; IV, intravenous.

Table 3
Parameter estimates of the best population PK model for biAP and recAP.

Parameter	Units	Typical value biAP (%RSE)	Typical value recAP (%RSE)	IIV (%)	Shrinkage (%)
CL	L/h	10.3 (10.1)	0.494 (4.11)	33.3[a]	5.5
V_1	L	8.30 (8.62)	4.22 (6.68)	32.2[a]	15.1
Q	L/h	11.8 (13.0)	7.36 (9.64)	55.2[a]	8.95
V_2	L	39.9 (26.3)	23.6 (5.36)	–	–
c_0	ng/mL	4.73 (5.75)	–	–	–
$t_{1/2\alpha}$[b]	h	0.25	0.32		
$t_{1/2\beta}$[b]	h	5.3	41.2		
Proportional error	0.0788				

[a] Estimated species-independently.
[b] Derived parameter. c_0, baseline concentration; IIV, inter-individual variability derived by 100*sqrt(exp(ω^2) – 1), where ω^2 is the variance of IIV; RSE, relative standard error derived by standard error/estimate × 100%.

of quantification were removed from the data set (>25% per subset) (Ahn et al., 2008). For the separate translational PK models for biAP and recAP, two-compartmental models with proportional error and inter-individual variability on CL best described the observed data. For biAP, a quantifiable baseline concentration was identified in the initial assessment of the data for which was corrected accordingly (c_0). Allometric scaling based on body weight (Eq. (1)) allowed accurate description of the PK observations in all species. The best model describing both biAP and recAP data simultaneously was therefore also parameterized in terms of CL, volume of distribution of the central compartment (V_1), intercompartmental exchange (Q) and volume of distribution of the peripheral compartment (V_2). A proportional error structure best described the residual error. This model was extended by (species-independent) inter-individual random effects to CL, V_1 and Q, as the OFV decreased with 197, 98 and 115 points respectively. Consecutive inclusion of a full variance covariance matrix to these three parameters improved the OFV by 33 points and was therefore kept in the best model structure. The parameter estimates obtained are summarized in Table 3. Values for RSE and shrinkage were all well within the acceptance criteria. The goodness-of-fit plots are represented in Fig. 3. The population predicted versus observed concentrations plot indicates that the model is structurally sound, as the observations are mostly centred around the line of unity. After inclusion of inter-individual variability (individual predictions, IPRED) the observations are more closely aligned to the line of unity, indicating improved descriptive properties. The CWRESI is close to being normally distributed around zero for the entire concentration range, indicating no bias for specific concentration ranges. Also for CWRESI over time clear bias is absent, although there are a few outliers outside the acceptance criterion. The frequency distribution of the CWRESI was slightly skewed to the right, the frequency distributions for the inter-individual variability parameters closely approached normal distributions (data not shown). From the correlation plots, a statistically significant relation between dose vs. IIV of V_1 and dose vs. IIV on Q was found (r^2: 0.32 and 0.34, respectively), hinting towards nonlinearity of AP, as did the results from the non-compartmental analysis. Therefore, a nonlinear Michaelis–Menten kinetics model was fitted to the data. The goodness-of-fits plots did not improve as was also

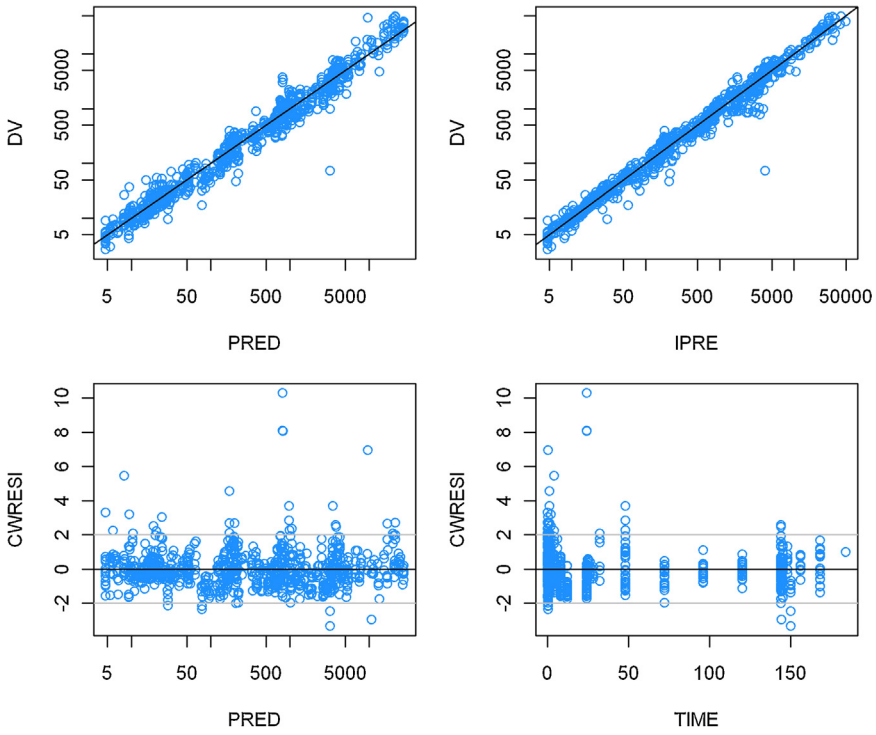

Fig. 3. Goodness of fits plots. Upper left: observed (DV) versus population predicted (PRED) concentrations, with a line of unity (black). Upper right: DV versus individual predicted concentrations (IPRE) with a line of unity (black). Lower left: conditional weighted residuals (CWRESI) versus population predicted concentrations (PRED), with acceptance criterion (grey line). Lower right: CWRESI versus time (TIME), with acceptance criterion (grey line).

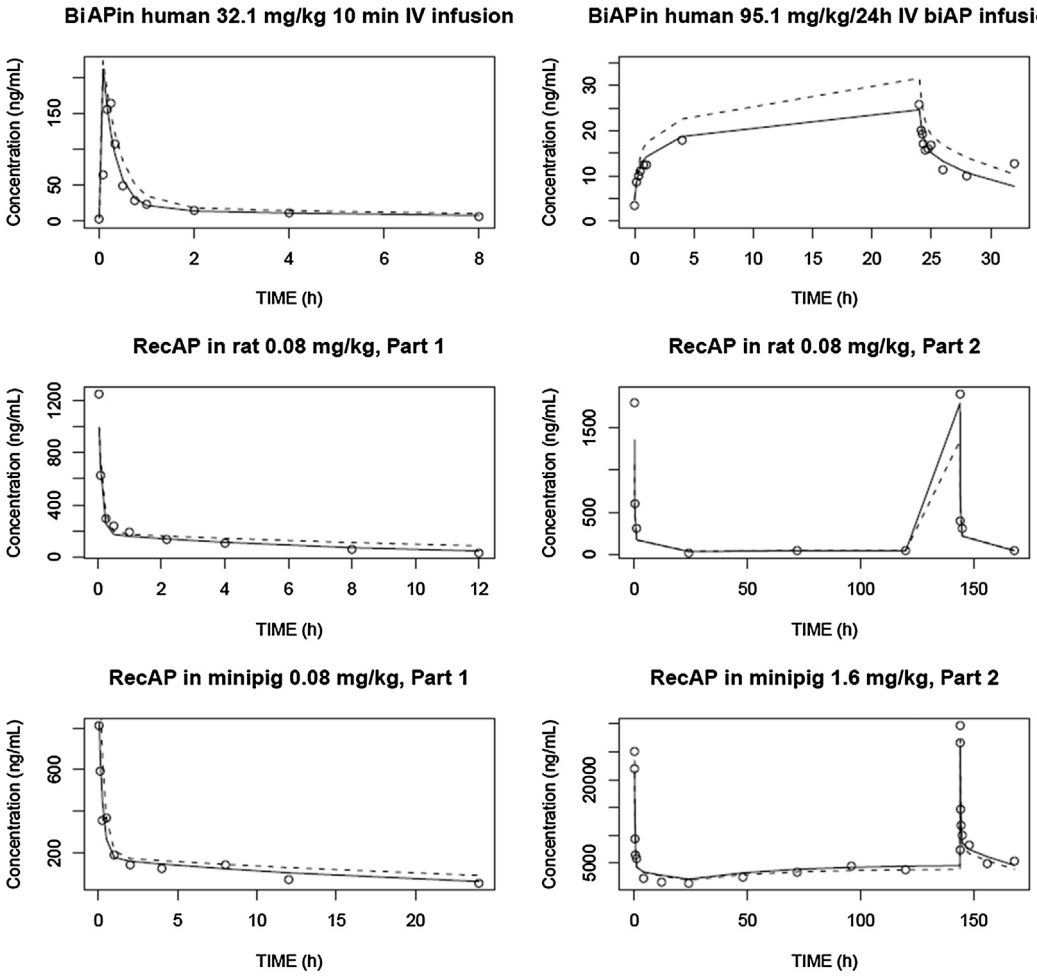

Fig. 4. Model performance on individual level. Individual predicted (solid line), population predicted (dotted line) and observed (open circles) plasma recAP/biAP concentrations over time. Per species, one typical individual is depicted for both a single and multiple dosing regimen. Part 1 represents the single dose regime, Part 2 represents the multiple dose regimen.

concluded from the lack in improvement in fit (ΔOFV; −5.33). The estimated Km was approximately 20-fold higher than the highest observed concentration, and the coefficient of variation of K_m and V_{max} was >75%. The high uncertainty in the population parameter estimates resulted in overparameterization when attempts were made to add IIV on any of the parameters. Applying nonlinear PK to recAP or BiAP separately did also not improve the model fits. These results clearly indicate that the concentration range of the data lies within the range of the Michaelis–Menten elimination rate-concentration relationship that approaches a linear relationship. Hence, a nonlinear model approach was abandoned. Fig. 4 represents individual predictions and population predictions with their actual data points, for typical individuals from each species dataset. For biAP administered to humans, both the observed data after a short 10 min infusion as well as the data after 24 h IV infusion are well described. The same accounts for recAP after single- and multiple-dose administration. These results indicate that kinetics of both biAP and recAP are accurately described by the two-compartmental population PK model with allometric scaling based on body weight.

4. Discussion

In this study, we successfully developed a translational population PK model of recAP to support the design and selection of dose levels to be investigated in the first-in-man trial as novel treatment strategy of sepsis-associated AKI. RecAP was developed as a suitable alternative to bovine-sourced intestinal AP, which was previously demonstrated to improve renal function in critically ill patients with sepsis-associated AKI (Pickkers et al., 2012). In addition, we performed an animal study to investigate the tissue distribution of recAP in vivo. Rats received LPS (or placebo) to induce systemic inflammation and, subsequently, endotoxemia-induced AKI, to assess the pharmacokinetic behavior of recAP in a preclinical model more closely representing the targeted patient population. After two hours, when systemic inflammation reached its peak (Pickkers et al., 2006), ^{125}I-labeled recAP was injected, and at several time-points radioactivity levels in diverse tissues were determined. As circulating AP is normally cleared through uptake by the hepatic asialoglycoprotein receptor (Blom et al., 1998; Tuin et al., 2006), the liver was the major site of accumulation and removal of ^{125}I-recAP; most radioactivity was captured by this organ within 10 min after injection and disappeared after two to four hours. In addition, spleen, adrenal gland, heart, lung and kidney showed uptake shortly after ^{125}I-recAP infusion, followed by the gastro-intestinal tract and thyroid gland. The presence of radioactivity in intestines can be explained by a fast distribution of ^{125}I-recAP into the liver and subsequent excretion into the intestine via bile (enterohepatic circulation). The ductus choledochus ends at the beginning of the duodenum. As the duodenum is in close proximity to the stomach, the stomach would have to be dissected carefully by an incision through the pyloric sphincter in

order to assess the relative importance of enterohepatic circulation versus distribution to the stomach. Macroscopically during dissection we could not distinguish the pyloric sphincter from the duodenum, therefore enterohepatic circulation cannot be excluded as a possible explanation for the observed radioactivity in the stomach.

Furthermore, serum recAP radioactivity and AP enzyme activity levels were significantly higher directly after ^{125}I-recAP injection in endotoxemic rats compared to healthy rats, as was the radioactive content in the heart. These differences are likely to be explained by LPS-induced reduction of the mean arterial blood pressure, which is known to occur in this model within one hour after the induction of endotoxemia (Kox et al., 2012). Beyond these observed differences, endotoxemia did not critically affect the ^{125}I-recAP tissue distribution and enzymatic terminal half-life.

Single and multiple doses of recAP (50, 200 or 1000 U/kg) were administered to rats and minipigs. Repeated dosing was well tolerated, without significant accumulation or discernible effects on morbidity, mortality and clinical observations, indicating that in these species repeated dosing of recAP could be done without any safety concerns. Both plasma recAP concentrations and AP enzymatic activity increased with increasing recAP dose and disappeared in a biphasic manner. With respect to dose-proportionality, C_{max} increased in proportion to dose over the entire dose range in nearly all protocols after non-compartmental analysis, while AUC increased slightly more than dose-proportional between the lowest and middle dose, and in proportion to dose between the middle and highest dose. In accordance, plasma clearance was higher at the lowest dose compared to the middle and highest dose, possibly suggesting that recAP PK was more affected by liver uptake mechanisms at the lowest dose level tested.

Subsequently, a two-compartmental translational population PK model with allometric scaling based on body weight was developed that accurately described both the PK of biAP and recAP. Due to lack of specificity of the AP enzyme activity assay, biAP data required correction for baseline endogenous AP circulating in the plasma. The inability to separate endogenous enzyme activity from exogenously added biAP may be causative to the increased uncertainty (%RSE) of biAP PK parameters compared to recAP parameters. After non-compartmental analyses, we observed a slight under-estimation at the highest dose levels versus population prediction, which indicates that first-order elimination might not be valid at that dose range. However, it might be attributed to random effects due to the small number of subjects in the highest dose group. Because inclusion of nonlinear kinetics did not improve the prediction at these dose levels, we did not include nonlinear elimination in the model. Furthermore, biAP was rapidly eliminated from dosed volunteers, presumably by the asialoglycoprotein receptor on liver cells (Blom et al., 1998). The high degree of sialylation of recAP could increase the terminal half-life of recAP, which is in agreement with the approximately 7.8-fold increase of apparent terminal half-life comparing recAP to biAP. The remaining PK parameters were in the same order of magnitude compared to biAP, confirming that the difference in PK profile between recAP and biAP should be attributed mainly to a difference in clearance rate.

In conclusion, the results presented in this study indicate that the tissue distribution of recAP is not critically affected by endotoxemia. In addition, we generated a translational two-compartmental model with allometric scaling based on body weight that can be used to simulate the predicted human plasma PK profile for different recAP dosing regimens. This model is expected to provide valuable insights into the choice of dosing scheme and dose levels for the first-in-man trial of recAP, essentially contributing to the clinical development of recAP as a potential new treatment option for sepsis-associated AKI.

Conflict of interest

P Pickkers received speaking and consultation fees from AM-Pharma, which developed the bovine intestinal AP and human recombinant AP therapeutics. A van Elsas received consultancy fees from AM-Pharma. J Arend and W Raaben are employees of AM-Pharma. The remaining authors declare that they have no relevant financial interests.

Author contribution

Participated in research design: Peters, Arend, Raaben, Elsas, Masereeuw, Pickkers Conducted experiments: Peters, Arend, Raaben Contributed new reagents or analytic tools: Laverman Performed data analysis: Peters, Stevens, Guan, Raaben, Masereeuw Wrote or contributed to the writing of the manuscript: Peters, Stevens, Arend, Guan, Raaben, Laverman, Elsas, Masereeuw, Pickkers All authors read and approved the final manuscript.

Acknowledgements

We are grateful to Bianca Lemmers-van de Weem, Kitty Lemmens-Hermans, Iris Lamers-Elemans and Henk Arnts (Preclinical Image Centre, Radboudumc) for their excellent technical assistance.

Appendix A. Supplementary data

Supplementary data associated with this article can be found, in the online version, at http://dx.doi.org/10.1016/j.ijpharm.2015.08.090.

References

Ahn, J.E., Karlsson, M.O., Dunne, A., Ludden, T.M., 2008. Likelihood based approaches to handling data below the quantification limit using NONMEM VI. J. Pharmacokinet. Pharmacodyn. 35, 401–421.
Berg, D.T., Gupta, A., Richardson, M.A., O'Brien, L.A., Calnek, D., Grinnell, B.W., 2007. Negative regulation of inducible nitric-oxide synthase expression mediated through transforming growth factor-beta-dependent modulation of transcription factor TCF11. J. Biol. Chem. 282, 36837–36844.
Beumer, C., Wulferink, M., Raaben, W., Fiechter, D., Brands, R., Seinen, W., 2003. Calf intestinal alkaline phosphatase, a novel therapeutic drug for lipopolysaccharide (LPS)-mediated diseases, attenuates LPS toxicity in mice and piglets. J. Pharmacol. Exp. Ther. 307, 737–744.
Blom, E., Ali, M.M., Mortensen, B., Huseby, N.E., 1998. Elimination of alkaline phosphatases from circulation by the galactose receptor. Different isoforms are cleared at various rates. Clin. Chim. Acta Int. J. Clin. Chem. 270, 125–137.
Boxenbaum, H., 1982. Interspecies scaling, allometry, physiological time, and the ground plan of pharmacokinetics. J. Pharmacokinet. Biopharm. 10, 201–227.
Cohen, J., 2002. The immunopathogenesis of sepsis. Nature 420, 885–891.
Coux, G., Trumper, L., Elias, M.M., 2002. Renal function and cortical (Na(+)+K(+))-ATPase activity, abundance and distribution after ischaemia-reperfusion in rats. Biochim. Biophys. Acta 1586, 71–80.
Eltzschig, H.K., Sitkovsky, M.V., Robson, S.C., 2012. Purinergic signaling during inflammation. New Engl. J. Med. 367, 2322–2333.
EMA, 2007. Committee for Medical Products for Human use. Guideline on Reporting the Results of Population Pharmacokinetic Analyses. European Medicines Agency, Londen.
FDA, 1999. Population PK working group. Guidance for Industry: Population Pharmacokinetics.
Greenwood, F.C., Hunter, W.M., Glover, J.S., 1963. The preparation of I-131-labelled human growth hormone of high specific radioactivity. Biochem. J. 89, 114–123.
Heemskerk, S., Masereeuw, R., Moesker, O., Bouw, M.P., van der Hoeven, J.G., Peters, W.H., Russel, F.G., Pickkers, P., Group, A.S., 2009. Alkaline phosphatase treatment improves renal function in severe sepsis or septic shock patients. Crit. Care Med. 37 (417–423), e411.
Heemskerk, S., Pickkers, P., Bouw, M.P., Draisma, A., van der Hoeven, J.G., Peters, W.H., Smits, P., Russel, F.G., Masereeuw, R., 2006. Upregulation of renal inducible nitric oxide synthase during human endotoxemia and sepsis is associated with proximal tubule injury. Clin. J. Am. Soc. Nephrol. CJASN 1, 853–862.

Khundmiri, S.J., Asghar, M., Khan, F., Salim, S., Yusufi, A.N., 1997. Effect of reversible and irreversible ischemia on marker enzymes of BBM from renal cortical PT subpopulations. Am. J. Physiol. 273, F849–856.
Kiffer-Moreira, T., Sheen, C.R., Gasque, K.C., Bolean, M., Ciancaglini, P., van Elsas, A., Hoylaerts, M.F., Millan, J.L., 2014. Catalytic signature of a heat-stable, chimeric human alkaline phosphatase with therapeutic potential. PLoS One 9, e89374.
Kox, M., Vaneker, M., van der Hoeven, J.G., Scheffer, G.J., Hoedemaekers, C.W., Pickkers, P., 2012. Effects of vagus nerve stimulation and vagotomy on systemic and pulmonary inflammation in a two-hit model in rats. PLoS One 7, e34431.
Lalles, J.P., 2014. Intestinal alkaline phosphatase: novel functions and protective effects. Nutr. Rev. 72, 82–94.
Millan, J.L., 2006. Alkaline phosphatases: structure, substrate specificity and functional relatedness to other members of a large superfamily of enzymes. Purinergic Signal. 2, 335–341.
Oppert, M., Engel, C., Brunkhorst, F.M., Bogatsch, H., Reinhart, K., Frei, U., Eckardt, K. U., Loeffler, M., John, S., German Competence Network, S., 2008. Acute renal failure in patients with severe sepsis and septic shock–a significant independent risk factor for mortality: results from the German Prevalence Study. European Renal AssociationNephrology, Dialysis, Transplantation: Official Publication of the European Dialysis and Transplant Association, 23. , pp. 904–909.
Pearson, K., 1895. Note on regression and inheritance in the case of two parents. Proc. R. Soc. Lond. 58, 240–242.
Peters, E., Heemskerk, S., Masereeuw, R., Pickkers, P., 2014. Alkaline Phosphatase: A Possible Treatment for Sepsis-Associated Acute Kidney Injury in Critically Ill Patients. Am. J. Kidney Dis. Off. J. Natl. Kidney Found..
Pickkers, P., Dorresteijn, M.J., Bouw, M.P., van der Hoeven, J.G., Smits, P., 2006. In vivo evidence for nitric oxide-mediated calcium-activated potassium-channel activation during human endotoxemia. Circulation 114, 414–421.
Pickkers, P., Heemskerk, S., Schouten, J., Laterre, P.F., Vincent, J.L., Beishuizen, A., Jorens, P.G., Spapen, H., Bulitta, M., Peters, W.H., van der Hoeven, J.G., 2012. Alkaline phosphatase for treatment of sepsis-induced acute kidney injury: a prospective randomized double-blind placebo-controlled trial. Crit. Care 16, R14.
Pickkers, P., Snellen, F., Rogiers, P., Bakker, J., Jorens, P., Meulenbelt, J., Spapen, H., Tulleken, J.E., Lins, R., Ramael, S., Bulitta, M., van der Hoeven, J.G., 2009. Clinical pharmacology of exogenously administered alkaline phosphatase. Eur. J. Clin. Pharmacol. 65, 393–402.
R, DCT, 2010. A Language and Environment for Statistical Computing. The R Foundation for Statistical Computing, Vienna, Austria.
Su, F., Brands, R., Wang, Z., Verdant, C., Bruhn, A., Cai, Y., Raaben, W., Wulferink, M., Vincent, J.L., 2006. Beneficial effects of alkaline phosphatase in septic shock. Crit. Care Med. 34, 2182–2187.
Tuin, A., Huizinga-Van der Vlag, A., van Loenen-Weemaes, A.M., Meijer, D.K., Poelstra, K., 2006. On the role and fate of LPS-dephosphorylating activity in the rat liver. Am. J. Physiol. Gastr. Liver Physiol. 290, G377–G385.
van Veen, S.Q., van Vliet, A.K., Wulferink, M., Brands, R., Boermeester, M.A., van Gulik, T.M., 2005. Bovine intestinal alkaline phosphatase attenuates the inflammatory response in secondary peritonitis in mice. Infect. Immun. 73, 4309–4314.
Verweij, W.R., Bentala, H., Huizinga-van der Vlag, A., Miek van Loenen-Weemaes, A., Kooi, K., Meijer, D.K., Poelstra, K., 2004. Protection against an *E. coli*-induced sepsis by alkaline phosphatase in mice. Shock 22, 174–179.